Far-infrared upconversion imaging devices: Imaging characteristics and quantum efficiency

L. K. Wu and W. Z. Shen[a)]
Laboratory of Condensed Matter Spectroscopy and Opto-Electronic Physics, Department of Physics, Shanghai Jiao Tong University, 1954 Hua Shan Road, Shanghai 200030, People's Republic of China

(Received 21 April 2006; accepted 12 July 2006; published online 23 August 2006)

We have carried out an investigation of imaging characteristics and quantum efficiency of far-infrared (FIR) semiconductor imaging devices. The realization of the FIR imaging employs the concept of photon frequency upconversion in GaAs homojunction interfacial work-function internal photoemission (HIWIP) FIR detectors integrated with GaAs/AlGaAs near-infrared light-emitting diodes (LEDs). Satisfying images have been expected through the analysis of modulation transfer function of the system, where the FIR detector parameters play key roles in the low spatial frequency image contrast, while those of LEDs dominate in the high spatial frequency range. We have examined in detail the dependence of the quantum efficiency on the emitter layer number, thickness, doping concentration, and applied bias of the FIR detectors, as well as the active layer thickness and internal quantum efficiency of the LEDs. The present study has also yielded an optimal structure for the integrated HIWIP-LED FIR imaging devices. © *2006 American Institute of Physics*. [DOI: 10.1063/1.2335599]

I. INTRODUCTION

Far-infrared (FIR)/terahertz electromagnetic radiation and detection have received more and more attention nowadays due to their potential applications in various areas, such as biomedical imaging, space astronomy, quantum computing, spectroscopy, and communications.[1–4] The recent rapid progress in mature GaAs quantum cascade lasers[5] (QCLs) can foresee the realization of commercial FIR/terahertz semiconductor sources. However, up to now, the study on the mature semiconductor FIR/terahertz detectors is still at early stage, with the primary commercially available thermal detectors of bolometers and pyroelectrics. Recently, FIR detection concept has been proposed based on the internal photoemission through the difference of work functions at semiconductor homojunction interfaces.[6] The corresponding GaAs homojunction interfacial work-function internal photoemission (HIWIP) FIR detectors[7] with resonant-cavity-enhanced effect[8] have been fabricated and demonstrated successfully. The unique feature of the HIWIP FIR detectors is that the cutoff wavelength (λ_c) is tailorable (via doping concentration and bias) and covers several tens to a few hundreds of micrometers.

For detection imaging, the concept of the photon frequency upconversion, which was proposed and realized in Ge/GaAs heterojunction in 1960s,[9] provides the possibility for converting the arbitrary wavelength light into short wavelength light that falls into the efficient imaging range of conventional silicon (λ_c about 1 μm) charged coupled devices (CCD). In 1995, Liu *et al.* successfully fabricated an upconversion device: quantum well infrared photodetector (QWIP) epitaxially integrated with a light-emitting diode (LED).[10] Upon midinfrared (MIR) illumination the resistance of the QWIP is decreased and, therefore, an additional voltage is applied across the LED which leads to an increase of the shorter wavelength light emission of the LED. Such an optical upconverter combined with a Si CCD could convert the MIR radiation into near-infrared (NIR) signal to realize MIR detection imaging. The QWIP-LED upconverter is not necessarily separated into pixels due to the sufficient number of QWs in QWIP (Ref. 11) and avoids the conventional silicon readout circuit hybridization for detection imaging, so it could bring down the cost of IR imaging. Ryzhii *et al.* have further investigated in detail the detection imaging of QWIP-LED,[11] photon recycling effect in LED,[12,13] and photonic breakdown in QWIP,[14] in order to clearly understand the IR imaging mechanism and improve the performance of the QWIP-LED upconverters.

There are two requirements to obtain image with negligible distortion and cross-talk in upconverting devices.[10] One is that the entire active part of the imaging system must be thin, and the other is that the motion of photoexcited carriers in the plane perpendicular to the electric field should be small. Due to the diffraction limit, these two requirements can be met when the thickness of the active part and the perpendicular motion are less than the IR wavelength. With the further increase of the IR wavelength, these two requirements should be easily satisfied. This opens options for developing semiconductor FIR imaging devices by integrating the GaAs HIWIP FIR detector with a GaAs/AlGaAs NIR LED, together with the advantage of the mature and uniform GaAs material growth and monolithic integration technology. In this paper, we have carried out a detailed investigation of imaging characteristics and quantum efficiency in HIWIP-LED FIR imaging devices and provided optimal device parameters for the FIR to NIR upconverter.

[a)]Author to whom correspondence should be addressed; electronic mail: wzshen@sjtu.edu.cn

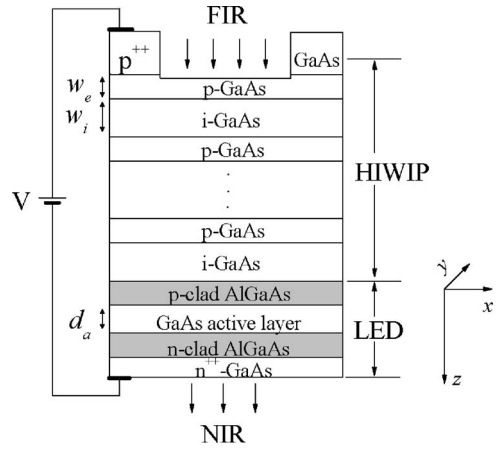

FIG. 1. Schematic view of the cross section of an integrated HIWIP-LED FIR to NIR upconverter.

II. THEORETICAL BACKGROUND

Figure 1 shows a schematic view of a HIWIP-LED integrated device and its operating principle. In addition to the bottom contact n^{++}-GaAs layer, the HIWIP FIR detector includes the top p^{++}-GaAs contact layer, periodic structures of heavily doped p-GaAs emitter layer, and intrinsic i-GaAs layer, while the double heterostructure LED consists of a narrow-gap GaAs active layer sandwiched between two wide-gap confining n- and p-AlGaAs layers. w_e, w_i, and d_a are the thicknesses of the GaAs emitter layer, intrinsic layer, and GaAs active layer, respectively, and V is the applied forward bias.

The absorption mechanism involved in the GaAs HIWIP FIR detector is free carrier absorption, which mainly occurs in the heavily doped p-GaAs emitter layers. Under the FIR radiation, holes are photoexcited from the low energy states to high ones of the valence band and diffuse to the emitting interfaces with the transport probability determined by the diffusion length. Then, those reaching the emitting interfaces tunnel through the interfacial barriers, which are due to the offset of the valence band edge caused by the band gap narrowing effect, and are collected by the image force at the interfaces to generate photocurrent.[6] The photoexcited holes past the HIWIP FIR detector are injected into the LED active region. Due to the confinement of wide-gap n- and p-AlGaAs layers, most of the holes recombine there, leading to the emission of NIR light through the radiative recombination.

In real LED structures, as a result of total internal reflection, only a small number of NIR photons generated escape, most of them are trapped in the LED, propagating along the HIWIP-LED plane. The trapped photons will be reabsorbed by the carriers and reemitted in the active layer, this reincarnation process is called photon recycling, which results in the enhancement of the external quantum efficiency of the LED (Ref. 13) and remarkable image distortion[12] (since the holes can appear far beyond the current injection area, well past the distances determined by the usual diffusion).

For the simplicity of the theoretical treatments, we neglect the impurity compensation in the p-GaAs emitter layers, the carrier diffusion along the axis z, and the carrier drift along axes x and y. Since the GaAs HIWIP FIR detector works under very low temperature (~4 K), the rate of the thermionic hole emission can be ignored too. By assuming that the in-plane potential is uniform within the emitter layers and the transport along the axis z drifts with a constant velocity v, we have the current continuity equation of the hole transport in the HIWIP FIR detector,

$$\frac{\partial p}{\partial t} = D\left(\frac{\partial^2 p}{\partial x^2} + \frac{\partial^2 p}{\partial y^2}\right) - \frac{\partial (vp)}{\partial z} + \sum_{m=1}^{N} (-p_c vp + G\phi^{\text{in}})\delta(z - mL), \tag{1}$$

where p is the hole concentration in the continuum, D is the diffusion coefficient of the holes, p_c is the capture probability[15] of holes in the GaAs emitter layers, so the quantity $p_c vp$ is the rate of the hole capture, and $L = w_e + w_i$. Since w_e is usually much smaller than w_i (w_i=100 nm), it is reasonable to employ the representation of the emitter layer by a δ function, just like the case of QWIPs.[11] N is the number of periodic structure in the HIWIP FIR detector, mL represents the coordinate z of a certain emitter layer plane, ϕ^{in} is the photon flux of the incoming FIR light, $G\phi^{\text{in}}$ is the rate of holes photoexcited across the barriers, and G satisfies[7]

$$G = [1 - \exp(-2\alpha_p w_e)]\exp\left(-\frac{w_e}{l}\right)\exp\left(-\frac{x_b}{l_s}\right), \tag{2}$$

here α_p is the coefficient of free carrier absorption; $\alpha_p = 8.28 \times 10^{-16}\ \text{cm}^2 \times N_a$ (Ref. 7) with N_a the doping concentration of the p-GaAs emitter layers; $l = \sqrt{DL/v}$ is the characteristic diffusion length; x_b is the distance from the interface to the barrier maximum in the HIWIP FIR detector; $x_b = \sqrt{q/16\pi\varepsilon E}$ with q the unit charge, ε the dielectric constant of p-GaAs, and E the electric field; $l_s = 276 \pm 2$ Å (Ref. 7) is the hole scattering length in the image force well.

We assume a two-dimensional sine target with the radiation photon flux distribution $\phi^{\text{in}} = \phi_0^{\text{in}} + \phi_{\mathbf{f}}^{\text{in}} \cos 2\pi \mathbf{fr}$, with $\mathbf{r} = (x, y)$, ϕ_0^{in} the average photon flux of the incoming FIR radiation, f the spatial frequency, and $\phi_{\mathbf{f}}^{\text{in}}$ the signal part amplitude of the sine wave. As we know, the spatial frequency f is the reciprocal of the spatial period of a sine target, indicating how often the object repeats per unit distance, and the common reference unit for spatial frequency is the number of line pairs per millimeter (lp/mm). Due to the diffraction limit, only images with $f \leqslant f_{\lambda_{\text{in}}} = 1/\lambda_{\text{in}}$ can be resolved (λ_{in} is the wavelength of FIR light).[11] The photocurrent density $j = evp$, and p has the form $p = p_0 + p_{\mathbf{f}} \cos 2\pi \mathbf{fr}$, with p_0 the average hole concentration and $p_{\mathbf{f}}$ the signal part amplitude characterizing the spatial distribution of holes in the layer planes. $p_{\mathbf{f}}$ is a function of the coordinate z, and in the top layer plane $z = 0$, we have the boundary condition of $p_{\mathbf{f}}|_{z=0} = 0$, under which Eq. (1) in the steady state yields

$$j_0 = \frac{qG\phi_0^{\text{in}}}{p_c}, \tag{3}$$

$$j_{\mathbf{f}}|_{z=B} = qG\phi_{\mathbf{f}}^{\text{in}} \exp(-4\pi^2 l^2 f^2) \times \frac{1-(1-p_c)^N \exp(-4\pi^2 l^2 f^2 N)}{1-(1-p_c)\exp(-4\pi^2 l^2 f^2)}, \quad (4)$$

where j_0 is the average photocurrent density over the planes and $j_{\mathbf{f}}|_{z=B}$ is the signal part amplitude of the output current density at the bottom layer plane of the HIWIP FIR detector.

The output NIR radiation photon flux can be presented as $\phi^{\text{out}} = \phi_0^{\text{out}} + \phi_{\mathbf{f}}^{\text{out}} \cos 2\pi \mathbf{fr}$. By employing the analysis for the GaAs/AlGaAs NIR LED in Ref. 13, we have the average photon flux ϕ_0^{out} and signal part amplitude $\phi_{\mathbf{f}}^{\text{out}}$ after taking into account the photon recycling effect,

$$\phi_0^{\text{out}} = \frac{t(1-\sigma)\eta_{\text{int}} j_0}{q[1-\sigma(\alpha_1/\alpha_2)\eta_{\text{int}}]}, \quad (5)$$

$$\phi_{\mathbf{f}}^{\text{out}} = \frac{t(1-\sigma)\eta_{\text{int}} j_{\mathbf{f}}|_{z=B}}{q\{1+4\pi^2 l_d^2 f^2 - \sigma\eta_{\text{int}}[\alpha_1\alpha_2/(\alpha_2^2+4\pi^2 f^2)]\}}, \quad (6)$$

here t is the transmission coefficient of the untrapped photons, σ is the fraction of the NIR photons trapped in the LED due to the total internal reflection, η_{int} is the internal quantum efficiency of the LED, and l_d is the diffusion length of carriers in the GaAs active layer. $\alpha_1 = \alpha_a\Gamma$ and $\alpha_2 = \alpha_a\Gamma + \alpha_c(1-\Gamma)$, where α_a and α_c are the photon absorption coefficients for the active region and surrounding layers, respectively, and $\Gamma = d_a/(d_a+d_c)$ with d_a the thickness of the LED active layer and d_c the net thickness of other layers between the reflecting surfaces.

III. FIR IMAGING CONTRAST TRANSFER

We can employ the modulation transfer function (MTF) to analyze the FIR image transfer characteristics of the HIWIP-LED upconverter. The MTF represents the ratio of the image contrast $(\phi_{\mathbf{f}}^{\text{out}}/\phi_0^{\text{out}})$ to the object contrast $(\phi_{\mathbf{f}}^{\text{in}}/\phi_0^{\text{in}})$, as a function of the spatial frequency f. Therefore, it is of fundamental importance in the testing of imaging systems, since it describes the ability of a system to transfer the object contrast to the image. From Eqs. (3)–(6), the MTF of the HIWIP-LED upconverter $T(f)$ is given by

$$T(f) = \frac{\phi_{\mathbf{f}}^{\text{out}}/\phi_0^{\text{out}}}{\phi_{\mathbf{f}}^{\text{in}}/\phi_0^{\text{in}}} = p_c \exp(-4\pi^2 l^2 f^2) \times \frac{1-(1-p_c)^N \exp(-4\pi^2 l^2 f^2 N)}{1-(1-p_c)\exp(-4\pi^2 l^2 f^2)} \times \frac{1-\sigma\eta_{\text{int}}(\alpha_1/\alpha_2)}{1+4\pi^2 l_d^2 f^2 - \sigma\eta_{\text{int}}[\alpha_1\alpha_2/(\alpha_2^2+4\pi^2 f^2)]}. \quad (7)$$

Figure 2 displays the spatial frequency dependence of the MTF under several device parameters for an imcoming FIR radiation of $\lambda_{\text{in}} = 60\ \mu$m, where the spatial frequency we study is limited to the range of $f \leq f_{\lambda_{\text{in}}} \approx 16.7$ lp/mm due to the diffraction limit. Figures 2(a) and 2(b) present the effects of the capture probability p_c and number of periodic structure N in the GaAs HIWIP FIR detector on the MTF characteristics. It is clear that the FIR imaging quality will be improved with the increase of p_c and N. The increase in p_c corresponds to the decrease of the photocurrent density injected to the LED, but from Eqs. (3) and (4) the nonuniform photocurrent will decrease at a slower rate than the uniform one, leading to the enhancement of the image contrast. With the increase of N, the nonuniform photocurrent increases, while the uniform part keeps unchanged due to its independence of N, so the MTF increases too. However, to sustain the impact ionization process in the HIWIP FIR detector, the number of periodic structure cannot be increased infinitely.[16] The relationship between N and the device parameters is given by $2^{N-2}q^2 w_i \leq \varepsilon_0 A\Delta$, with Δ the work function, ε_0 the dielectric constant of vacuum, and A the optical window area, a theoretical estimate with appropriate parameters gives $N \leq 21$ as a limit.[7] Furthermore, the MTF does not depend on the emitter layer doping concentration N_a and thickness w_e of the HIWIP FIR detector, as well as the applied electric field.

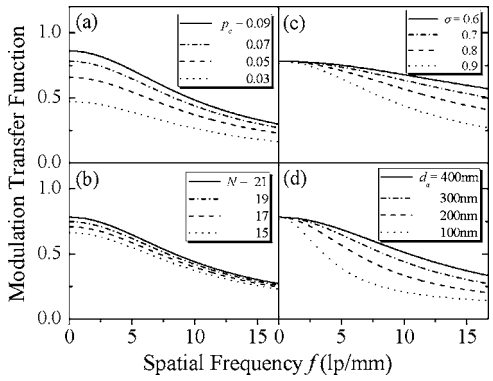

FIG. 2. Spatial frequency f dependence of modulation transfer function under various (a) capture probabilities p_c and (b) periodic structure numbers N of the GaAs HIWIP FIR detector, as well as (c) portions of trapped NIR photons σ and (d) active layer thicknesses d_a of the GaAs/AlGaAs NIR LED.

We show in Fig. 2(c) the dependence of the MTF on the fraction σ of the NIR photons trapped in the LED. With the increase of σ, more output NIR photons are trapped in the LED, which will be reabsorbed and reemitted. The photon recycling results in a smearing of the photocurrent spatial distribution and decrease of the MTF and image quality. In the case of small σ, the MTF drops slowly, where we can get satisfying image quality even at larger f. Nevertheless, the extraction efficiency of the LED is usually very low due to the total internal reflection, i.e., difficult to achieve small σ. Figure 2(d) gives the MTF as a function of the LED active layer thickness d_a. The results indicate that we can get better image contrast with the sufficiently large d_a. However, if d_a is too large, the number of photons trapped in the LED increases, leading to the increase of σ and the deterioration of the image. In addition, the internal quantum efficiency η_{int} of the LED also has effect on the MTF, as demonstrated in Ref. 13. The trapped photons could be reabsorbed and reemitted more efficiently with larger η_{int}, so the photon recycling effect is intensified, and the MTF decreases with the increase of η_{int}.

The above discussion allows us to achieve a set of optimal device parameters for both the HIWIP FIR detector and the LED: $p_c = 0.07$, $N = 21$, $\sigma = 0.9$, and $d_a = 300$ nm. It should be noted that the results (including those in the next section) have been calculated under the optimal parameters, except

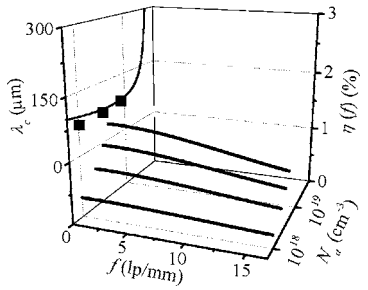

FIG. 3. Spatial frequency f dependence of signal quantum efficiency $\eta(f)$ at various emitter layer doping concentrations N_a, together with the theoretical N_a dependence of the cutoff wavelength λ_c and the experimental data (solid squares from Ref. 17).

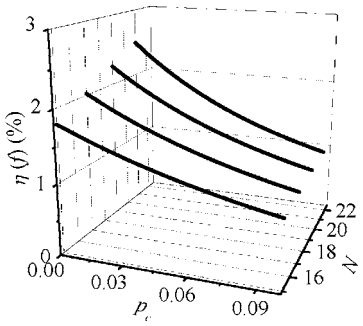

FIG. 4. Capture probability p_c dependence of $\eta(f)$ under several periodic structure numbers N.

for the examined one. It is well known that the image will not have perceived sharpness and resolution when $T(f)/T(0)$ is less than 0.5. We notice that our $T(f)/T(0)$ is always larger than 0.5 with these optimal parameters at a wide spatial frequency range of less than 13 lp/mm. Therefore, satisfying images can be expected in integrated HIWIP-LED FIR imaging devices. Furthermore, it is clear from Fig. 2 that the device parameters of the HIWIP FIR detector play key roles in the low spatial frequency image contrast, while those of the LED dominate in the high spatial frequency range.

IV. UPCONVERSION QUANTUM EFFICIENCY

Now, we move our attention to the signal quantum efficiency $\eta(f)$, which represents the rate of FIR photons converted into NIR photons and reflects the brightness of the image. Using Eqs. (2), (4), and (6), we obtain

$$\eta(f) = \frac{\phi_{\mathbf{f}}^{\text{out}}}{\phi_{\mathbf{f}}^{\text{in}}} = [1-\exp(-2\alpha_p w_e)]\exp\left(-\frac{w_e}{l}\right) \times \exp\left(-\frac{x_b}{l_s}\right)\frac{1-(1-p_c)^N\exp(-4\pi^2 l^2 f^2 N)}{1-(1-p_c)\exp(-4\pi^2 l^2 f^2)} \times \frac{t(1-\sigma)\eta_{\text{int}}}{1+4\pi^2 l_d^2 f^2 - \sigma\eta_{\text{int}}[\alpha_1\alpha_2/(\alpha_2^2+4\pi^2 f^2)]} \times \exp(-4\pi^2 l^2 f^2). \quad (8)$$

We start with the spatial frequency dependence of $\eta(f)$ under different emitter layer doping concentrations N_a of the GaAs HIWIP FIR detector. Figure 3 shows that $\eta(f)$ decreases with the increase of the spatial frequency f. In other words, the image brightness decreases with the decreasing size of the image details, in good agreement with the above MTF analysis that the image quality is not so satisfying in the high spatial frequency range. Simultaneously, with the increase of N_a, there are more holes in the emitter layers photoexcited by the FIR radiation, resulting in the increase of the number of output NIR photons. Therefore, $\eta(f)$ increases with N_a.

However, in the GaAs HIWIP FIR detector, N_a cannot be increased arbitrarily, it is restricted by the Mott transition concentration, under which semiconductor changes into metal. Neglecting the impurity compensation in the emitter layers, the Mott transition value in p-GaAs is 5.02×10^{19} cm^{-3}.[6] For the HIWIP FIR detector, the cutoff wavelength (λ_c) ties up with N_a. We have calculated, also shown in Fig. 3, the dependence of λ_c on N_a (in logarithm coordinate) by using the high density theory,[6] together with the experimental λ_c by solid squares.[17] It can be seen that there is a convincing agreement between the experimental data and calculated results, indicating clearly that the cutoff wavelength is tailorable through the change of N_a. In the following discussion, we choose $N_a=4\times10^{18}$ cm^{-3}, corresponding to λ_c of 60–100 μm (the variation of λ_c is due to different applied electric fields), where we will study the upconversion of 60 μm FIR radiation into NIR light at a characteristic spatial frequency of 5 lp/mm.

Figure 4 presents the dependence of $\eta(f)$ on the capture probability p_c and periodic structure number N. It is clear that $\eta(f)$ decreases with increasing p_c. Since the GaAs HIWIP FIR detector works under very low applied bias, we could expect that p_c does not show obvious dependence on bias. The drop in $\eta(f)$ is due to the decrease of the nonuniform photocurrent density injected into the LED, as a result of the fact that more holes will be captured in the emitter layers at larger p_c. In contrast, the MTF analysis in Sec. III reveals that the FIR image contrast will be improved with the increase of p_c. We therefore choose the optimal p_c of 0.07 for the GaAs HIWIP FIR detector in the present study. As for the periodic structure number N, we can observe that, same as the MTF results, $\eta(f)$ also increases with N, due to the increase of the nonuniform photocurrent. It is thus natural to set $N=21$ as an optimal parameter in Sec. III.

Other two important parameters for the GaAs HIWIP FIR detectors are the emitter layer thickness w_e and the applied electric field E. The solid curves in Fig. 5 are the de-

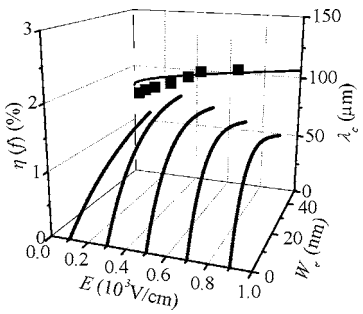

FIG. 5. Emitter layer thickness w_e dependence of $\eta(f)$ at various electric fields E. Also shown is the theoretical E dependence of the cutoff wavelength λ_c, together with the experimental results (solid squares from Ref. 7).

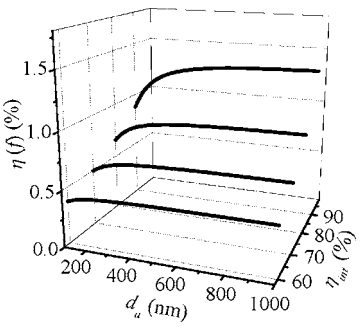

FIG. 6. Active layer thickness d_a dependence of $\eta(f)$ under various internal quantum efficiencies η_{int} of the GaAs/AlGaAs NIR LED.

pendences of $\eta(f)$ on w_e under different E. We can see that with increasing w_e, $\eta(f)$ increases first, then tends to saturate. This is due to the fact that when w_e is not too large, more holes in the GaAs emitter layers absorb FIR photons as w_e increases, resulting in the increase of the photocurrent density injected into the LED. When w_e is larger than the diffusion length of holes, only a fraction of holes contributes to the output current density, while others will be lost in the diffusion due to the scattering processes. A typical value of the hole diffusion length in p-GaAs is 20–30 nm,[7] so the thickness of the emitter layers is restricted by this value.

With the increase of electric field E, $\eta(f)$ exhibits a maximum at a certain value. The upper limit of the electric field corresponds to the case of the maximum responsivity of the GaAs HIWIP FIR detector, which is due to the possible impact ionization breakdown of neutral impurity atoms occurring in the intrinsic layers.[6] When E is larger than the upper limit, the dark current will increase rapidly, resulting in the decrease of the responsivity, which has been demonstrated experimentally.[18] In the HIWIP FIR detectors, the applied bias also decreases the image force barrier, leading to the increase of the cutoff wavelength λ_c. The electric field dependence of λ_c has also been calculated in Fig. 5, which agrees well with the experimental data shown by solid squares,[7] revealing the tunability of the cutoff wavelength by the applied electric field. The above arguments yield the appropriate values of $w_e=20$ nm and $E=0.3\times10^3$ V/cm in the GaAs HIWIP FIR detector to realize optimal upconversion of FIR radiation into NIR light.

We then discuss the roles of the LED device parameters in the signal quantum efficiency $\eta(f)$. Figure 6 displays the dependences of $\eta(f)$ on the two important parameters of the active layer thickness d_a and internal quantum efficiency η_{int}. It is clear that $\eta(f)$ exhibits saturation feature on d_a. Under narrow active layer, the photon recycling effect intensifies with the increase of d_a, where there are more NIR photons reabsorbed and reemitted, leading to the increase of $\eta(f)$. However, further increase of d_a will decrease the transmission coefficient of the NIR photons, which weakens the role of photon recycling and saturates $\eta(f)$.[13] The optimal value of d_a should be a tradeoff between the photon recycling effect and the decrease of transmission coefficient. Taking into account the relationship between the MTF and d_a shown in Fig. 2(d), it is reasonable for us to choose $d_a=300$ nm.

From Fig. 6, we observe that $\eta(f)$ increases with the LED internal quantum efficiency η_{int}. At high η_{int}, the bimolecular radiative recombination will dominate the recombination process, and the photon recycling effect is intensified, so $\eta(f)$ increases. Generally, the internal quantum efficiency of the GaAs/AlGaAs NIR LED could be achieved as high as 99.7%.[19] However, too high η_{int} will lead to the decrease of the MTF, as discussed in Sec. III, we therefore select 0.9 as a suitable value for η_{int} to achieve both sharp contrast and high signal quantum efficiency in the FIR upconversion imaging. In addition, we note that $\eta(f)$ is also closely related with the portion σ of the NIR photons trapped in the LED. The smaller σ corresponds to the higher extraction efficiency of the LED and therefore larger $\eta(f)$. Since the MTF also increases with decreasing σ, as shown in Fig. 2(c), it is of significant importance to improve the extraction efficiency of the GaAs/AlGaAs NIR LED to realize good FIR upconversion imaging.

Finally, it should be noted that with these optimal device parameters, the thickness of the total active part in the HIWIP-LED upconverter is about 0.7 μm, and the maximum perpendicular motion of photocarriers injected into the LED is estimated to be 0.4–0.6 μm. These two quantities are far less than the FIR wavelength and therefore will not result in obvious distortion and cross-talk in the FIR imaging. Since the trapped NIR photons can experience reemission, the quantum efficiency of the system has been improved by the photon recycling effect. Furthermore, the photocurrent injected into the GaAs/AlGaAs NIR LED is mainly due to the photoexcited holes and can almost maintain the spatial distribution of the FIR radiation, so the HIWIP-LED upconverter can serve as a pixel-less device.[10,11] Nevertheless, the diffusion length l_d of photocarriers in the LED is about 1 μm.[12] Due to the photon recycling effect, a NIR photon may experience 25 reincarnations in average before it escapes the LED.[19] The total diffusion length in the LED is about 25 μm, much larger than the smallest nonuniformity limited by diffraction ($1/2\pi f_{\lambda_{\text{in}}}\approx9.6$ μm), indicating that the photon recycling deteriorates the image quality. Simultaneously, the upconversion efficiency is still not high, similar to the QWIP-LED case in the range of 1%–3%,[20] mainly due to the low external quantum efficiency of the GaAs HIWIP FIR detector and low extraction efficiency of the GaAs/AlGaAs NIR LED. This can be implemented through the use of resonant-cavity-enhanced GaAs HIWIP FIR detector[8] and resonant microcavity LED (Ref. 21) to improve the efficiency of the HIWIP-LED FIR to NIR upconverter.

V. CONCLUSIONS

We have employed the photon frequency upconversion concept to investigate the semiconductor FIR imaging in a GaAs HIWIP FIR detector integrated with a GaAs/AlGaAs NIR LED, with the emphasis on the imaging characteristics and quantum efficiency. Through the analysis of the MTF, we could expect satisfying images in a wide spatial frequency range, where the low spatial frequency image contrast is dominated by the GaAs HIWIP FIR detector parameters, while LED ones govern the high frequency range. We have studied in detail several device parameters closely re-

lated to the signal quantum efficiency of the FIR to NIR upconverter and obtained the optimal structures for a FIR wavelength of 60 μm. From our experimentally demonstrated tailorable cutoff wavelength of the GaAs HIWIP FIR detector with both the emitter layer concentration and applied bias, it is clear that upconversion of longer FIR wavelength to NIR imaging is possible. Nevertheless, the efficiency of the HIWIP-LED integrated device still needs to be improved; the current study under way includes the theoretical analysis of the resonant-cavity-enhanced GaAs HIWIP FIR detector integrated with the resonant microcavity GaAs/AlGaAs NIR LED and the experimental demonstration of the HIWIP-LED FIR upconversion imaging.

ACKNOWLEDGMENTS

This work was supported by the Natural Science Foundation of China under Contract No. 60576067, Shanghai Municipal Commission of Science and Technology Project No. 05QMH1411, and the National Minister of Education Program for Changjiang Scholars and Innovative Research Team in University (PCSIRT).

[1]D. Arnone, C. Ciesla, and M. Pepper, Phys. World **13**, 35 (2000).
[2]B. E. Cole, J. B. Williams, B. T. King, M. S. Sherwin, and C. R. Stanley, Nature (London) **410**, 60 (2001).
[3]M. W. Werner, Infrared Phys. Technol. **35**, 539 (1994).
[4]L. Suvillaret, F. Garet, and J. L. Coutaz, Appl. Opt. **38**, 409 (1999).
[5]G. Scalari, L. Ajili, J. Faist, H. Beere, E. Linfield, D. Ritchie, and G. Davies, Appl. Phys. Lett. **82**, 3165 (2003).
[6]A. G. U. Perera, H. X. Yuan, and M. H. Francombe, J. Appl. Phys. **77**, 915 (1995).
[7]W. Z. Shen, A. G. U. Perera, H. C. Liu, M. Buchanan, and W. J. Schaff, Appl. Phys. Lett. **71**, 2677 (1997).
[8]Y. H. Zhang, H. T. Luo, and W. Z. Shen, Appl. Phys. Lett. **82**, 1129 (2003).
[9]P. W. Kruse, F. C. Pribble, and R. G. Schulze, J. Appl. Phys. **38**, 1718 (1967).
[10]H. C. Liu, J. Li, Z. R. Wasilewski, and M. Buchanan, Electron. Lett. **31**, 832 (1995); H. C. Liu, L. B. Allard, M. Buchanan, and Z. R. Wasilewski, *ibid.* **33**, 379 (1997).
[11]V. Ryzhii, H. C. Liu, I. Khmyrova, and M. Ryzhii, IEEE J. Quantum Electron. **33**, 1527 (1997).
[12]V. Ryzhii, I. Khmyrova, and Ph. Bois, IEEE J. Quantum Electron. **35**, 1693 (1999).
[13]N. Tsutsui, I. Khmyrova, V. Ryzhii, and T. Ikegami, Jpn. J. Appl. Phys., Part 1 **39**, 5080 (2000).
[14]V. Ryzhii and H. C. Liu, J. Appl. Phys. **92**, 2354 (2002).
[15]H. C. Liu, Appl. Phys. Lett. **60**, 1507 (1992).
[16]A. G. U. Perera, J.-W. Choe, M. H. Francombe, R. E. Sheriff, and R. P. Devaty, Superlattices Microstruct. **14**, 123 (1993).
[17]W. Z. Shen, A. G. U. Perera, M. H. Francombe, H. C. Liu, M. Buchanan, and W. J. Schaff, IEEE Trans. Electron Devices **45**, 1671 (1998).
[18]A. G. U. Perera, R. E. Sherriff, M. H. Francombe, and R. P. Devaty, Appl. Phys. Lett. **60**, 3168 (1992).
[19]I. Schnitzer, E. Yablonovitch, C. Caneau, and T. J. Gmitter, Appl. Phys. Lett. **62**, 131 (1993).
[20]E. Dupont, M. Byloos, M. Gao, M. Buchanan, C.-Y. Song, Z. R. Wasilewski, and H. C. Liu, IEEE Photonics Technol. Lett. **14**, 182 (2002).
[21]H. Chen, Z. Zou, C. Cao, and D. G. Deppe, Appl. Phys. Lett. **80**, 350 (2002).